

Article

Amphiboles from the garnet glaucophane schists in the Bizan area, Sambagawa metamorphic belt, eastern Shikoku, Japan

Md. Fazle Kabir* and Akira Takasu*

Abstract

The Sambagawa metamorphic belt in the Bizan area consists mainly of pelitic schists, basic schists, and siliceous schists, along with minor garnet glaucophane schists. Garnet glaucophane schists consist mainly of garnet and amphibole (glaucophane, ferroglaucophane, barroisite, katophorite and taramite), with minor amounts of epidote, phengite, paragonite, chlorite, albite, titanite, and quartz. Clinopyroxene (jadeite-omphacite), chloritoid, rutile, ilmenite, calcite, K-feldspar, zircon occur occasionally. Amphiboles have five modes of occurrence. Amphiboles inclusions in porphyroblastic garnets are sodic and sodic calcic amphiboles (Amp1; ferroglaucophane, glaucophane, ferrobarrroisite, barroisite, taramite). Taramitic amphiboles occur restrictedly in the cores of the porphyroblastic garnets. Amphibole inclusions in the rim of the garnets are zoned, with barroisite core and glaucophane rim. Amphibole inclusions in albite (Amp2), epidote (Amp3) and chlorite (Amp4) are ferroglaucophane in composition. Ferroglaucophane and glaucophane occur in the matrix (Amp5), and some of them are zoned from glaucophane core to barroisite rim. The diversity of the modes of occurrence and chemical compositions of the amphiboles reflect three metamorphic events of the garnet glaucophane schists in the Bizan area. A precursor metamorphic event is represented by the taramitic amphibole inclusions in the core of the porphyroblastic garnet. Schistosity-forming amphiboles (ferroglaucophane, glaucophane), amphiboles inclusions in the porphyroblastic garnets (ferroglaucophane, glaucophane, ferrobarrroisite, barroisite) and amphibols included in albite, epidote and chlorite (ferroglaucophane) are representative of the prograde to the peak metamorphism of eclogitic metamorphic event. Barroisite rim of zoned amphiboles is probably developed during the epidote-amphibolite metamorphic event.

Key words: Sambagawa (Sanbagawa) metamorphic belt, Bizan area, garnet glaucophane schist, eclogite, amphibole

Introduction

The Sambagawa metamorphic belt is a high-*P/T* type metamorphic belt that stretches through southwest Japan over a length of 800 km, from Saganoseki Peninsula in Kyushu to the Kanto Mountains in the east. The type of metamorphism is classified as high-pressure intermediate series (Miyashiro, 1973), and formed in a subduction-tectonic setting (e.g. Takasu *et al.*, 1994; Wallis, 1998). The dominant rock types within the belt are pelitic, psammitic, siliceous and basic schists that were derived from sedimentary rocks, and basaltic lavas and their derivatives. Metamorphic conditions within the belt correspond to the pumpellyite-actinolite, greenschist, blueschist, epidote-amphibolite and eclogite facies. In the Besshi district, the metamorphism is divided into four zones based on index minerals in pelitic schists (e.g. Higashino, 1975; 1990; Enami, 1983;). These are chlorite (300-360°C, 5.5-6.5 kbar), garnet (425-470°C, 7-8.5 kbar), albite-biotite (470-590°C, 8-9.5 kbar) and oligoclase-biotite (585-635°C, 9-11 kbar) zones (Enami, 1983; Enami *et al.*, 1994). A number of eclogite-bearing bodies are scattered throughout the albite and the oligoclase-biotite zones in the high-grade portions of the metamorphic sequence in the Besshi district, central Shikoku, such as the Higashi-akaishi and Nikubuchi peridotite bodies; the Western Iratsu, Quartz

Eclogite (Gongen), Seba eclogitic basic schists; Sebadani, Eastern Iratsu and Tonaru metagabbro masses (e.g. Kunugiza *et al.*, 1986; Takasu, 1989; Aoya, 2001; Ota *et al.*, 2004; Miyagi and Takasu, 2005; Miyamoto *et al.*, 2007; Kabir and Takasu, 2010a, b; Endo and Tsuboi, 2013).

The Bizan and the Kotsu areas are situated in the same tectonostratigraphic horizon, i.e. the Kotsu Formation in eastern Shikoku (Iwasaki, 1963; Kenzan Research Group, 1963) (Fig. 1). The Kawata Formation is composed of alternations of graphite-albite-quartz schists and albite-actinolite-epidote-chlorite schists, whereas the Kotsu Formation is composed of alteration of actinolite-epidote-chlorite schists and glaucophane-epidote-chlorite schists (Iwasaki, 1963). The Kawatayama Formation is composed chiefly of alternations of epidote-chlorite-actinolite schists and epidote-chlorite-glaucophane schists.

The main rock types in the Bizan area include pelitic, basic and siliceous schists with minor amounts of psammitic and calcareous schists (Iwasaki, 1963). Basic and pelitic schists show large-scale alternation, and siliceous schists occur as lenses or thin layers within the alterations. There is a tectonic mélange zone containing blocks of serpentinite, metagabbro and garnet-amphibolite (jadeite-bearing garnet-glaucophane schist in this study) that occurs along a ductile shear zone between the spotted and the non-spotted schist zones (Faure, 1983). The garnet glaucophane schists are usually found as lenticular bodies or layers ranging from centimeter to a few meters in thickness in pelitic schists that

*Department of Geoscience, Graduate School of Science and Engineering, Shimane University, 1060 Nishikawatsu, Matsue 690-8504, Japan

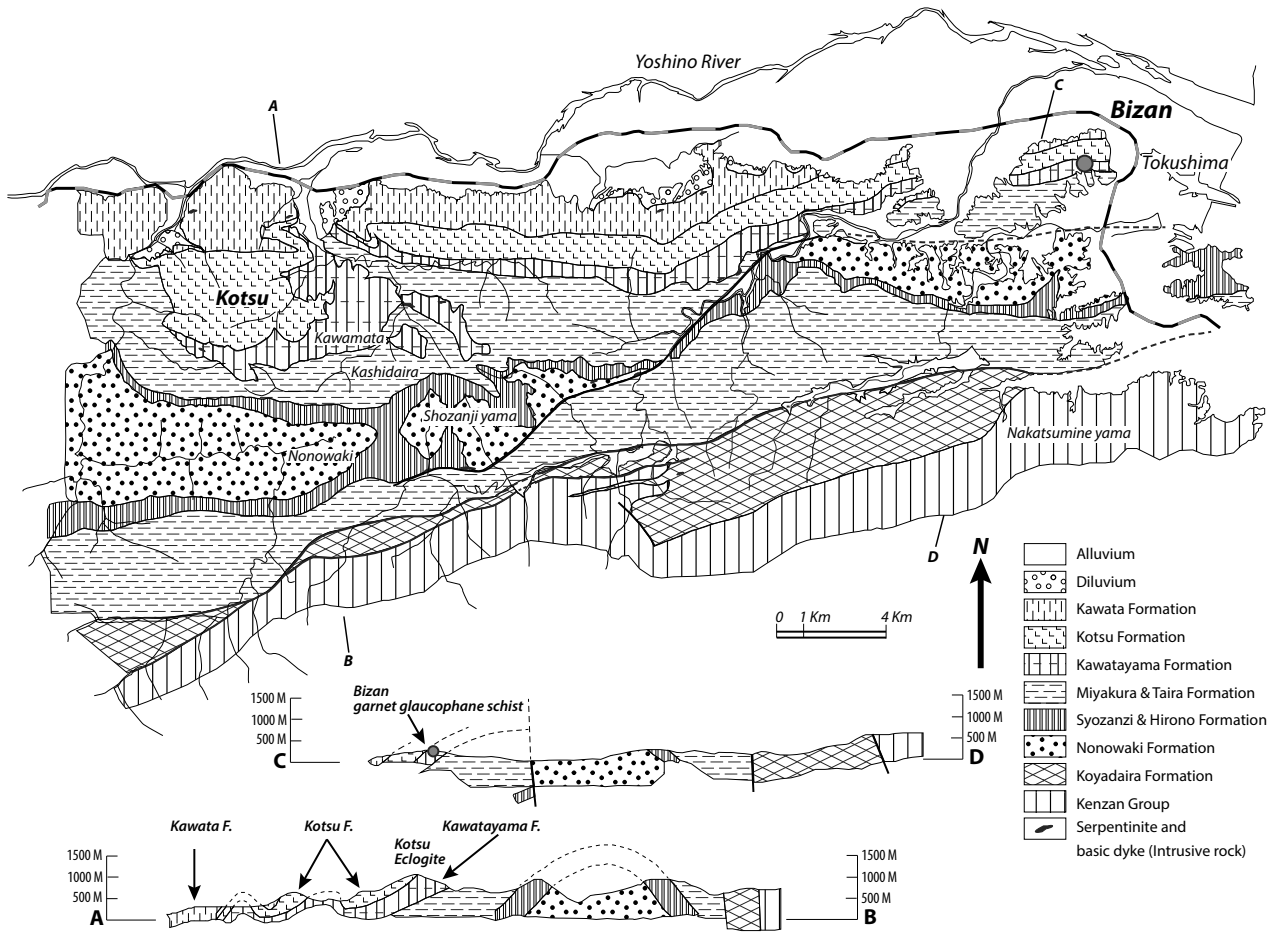


Fig. 1. Geological map of the Kotsu-Bizan area in eastern Shikoku, Sambagawa metamorphic belt (after Kenzan Research Group, 1963), and sample location.

crop out in the Chikurinji-dani valley (Fig. 1).

Iwasaki (1963) reported the occurrence glaucophane in the garnet-epidote-glaucophane schists from the Bizan area. In this study, we report the petrography of the garnet glaucophane schists, and describe the modes of occurrence and mineral chemistry of amphiboles within the garnet glaucophane schists. The mineral abbreviations used in the text, tables and figures follow Whitney and Evans (2010).

Petrography and mode of occurrence of amphiboles in the garnet glaucophane schists

Five garnet glaucophane schist samples from the Chikurinji dani Valley in the Bizan area were selected for detailed petrographic examination. Garnet glaucophane schists composed mainly of garnet and amphibole (glaucophane, ferroglaucophane, barroisite, katophorite and taramite). Minor amounts of epidote, phengite, paragonite, chlorite, albite, titanite, and quartz (Figs. 2 and 3). Clinopyroxene (jadeite-omphacite), chloritoid, rutile, ilmenite, calcite, K-feldspar, zircon occur as accessories. A schistosity is defined by preferred orientation of phengite and glaucophane (Fig. 2).

Porphyroblastic garnets occur as euhedral and subhedral

grains up to 6 mm across are optically zoned from pale orange core to colorless rim (Fig. 2 and 3a). The core of the garnets contains inclusions of amphibole, jadeite, epidote, phengite, paragonite, albite, chloritoid, chlorite, calcite, titanite, ilmenite, K-feldspar and quartz (Figs. 2 and 3a). The rim of the garnets contains inclusions of amphibole, jadeite, epidote, phengite, rutile, titanite, ilmenite and quartz (Fig. 3a-c). The porphyroblastic garnets are occasionally replaced by chlorite along their rim and crack. Clinopyroxenes (X_{Id} 0.46-0.75) occur as inclusions in garnet are of anhedral grain up to 0.03 mm across.

Amphiboles in the garnet glaucophane schists display five different modes of occurrence (Amp1-5). Amphiboles of Amp1 occur as inclusions in the porphyroblastic garnets. The amphibole inclusions in the cores of the garnets occur as subhedral prismatic crystals up to 2 mm long. They are sodic and sodic-calcic amphiboles (ferroglaucophane, glaucophane, ferrobarroisite, barroisite, taramite) (Fig. 3a-c). The rims of the garnets contain sodic and sodic-calcic amphiboles such as glaucophane and barroisite (Fig. 3b,c). Amphiboles are also included in albite (Amp2), epidote (Amp3) and chlorite (Amp4), and they are ferroglaucophane in composition (Fig. 3d-f). Amphibole inclusions in epidote

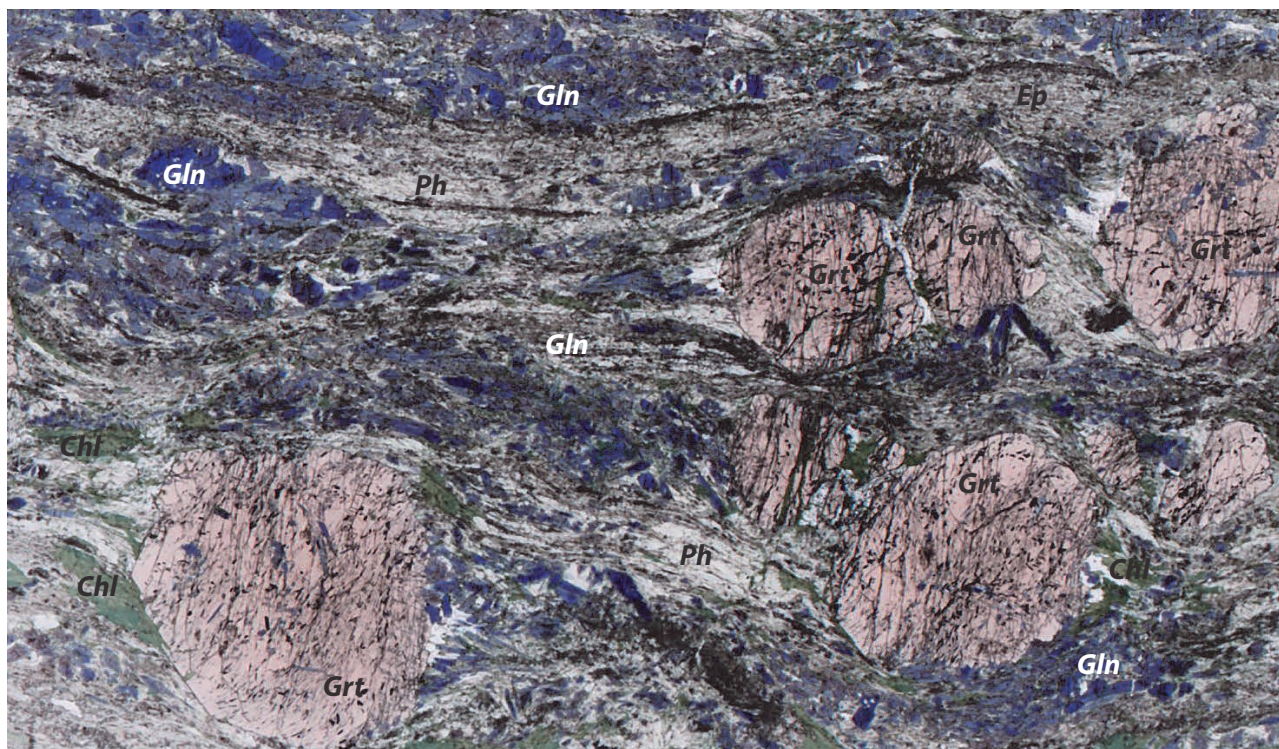


Fig. 2. Photomicrograph of the garnet glaucophane schists from the Bizan area showing porphyroblastic garnets and schistosity-forming matrix minerals of glaucophane (Amp5), phengite, epidote and chlorite. Porphyroblastic garnets contains plenty of inclusions, such as glaucophane (Amp1).

are fine grained, and inclusions in albite and chlorites are up to 0.8 mm across. Amphiboles (Amp5) are mostly ferroglaucophane and glaucophane occurring as subhedral to anhedral prismatic grains up to 4 mm long in the matrix (Figs. 2 and 3a). They contain inclusions of epidote, phengite, paragonite, chlorite, albite, titanite and quartz. Few barroisite, katophorite and taramite also occur in the matrix. Some amphiboles in the matrix are zoned from glaucophane core to barroisite rim. Amphiboles are partly replaced by albite and chlorite along the rim and the crack.

Chemical compositions of the amphiboles

Chemical compositions and zoning of the amphiboles in garnet glaucophane schists from the Bizan area were examined at Shimane University using two electron probe microanalyzers (JEOL JXA-8800M and JXA-8530F). Analytical conditions applied were 15 kV accelerating voltage, 20 nA specimen current and 5 μ m beam diameter. Correction procedure was carried out as described by (Bence and Albee, 1968). Fe^{3+} estimation for amphiboles used the 13eCNK method by Leake *et al.* (1997).

The chemical compositions of amphiboles are shown in Fig. 4. Amphiboles (Amp1) inclusions in the core of the porphyroblastic garnets are taramite, and have higher Al (Al_2O_3 11.32-16.21 wt%) and lower Si (6.14-6.44 pfu), Na_B (0.53-0.99) and X_{Mg} (Mg/Mg+ Fe^{2+}) (0.11-0.49) (Fig. 4c;

Table 1). Amphiboles (Amp1) included in the core and the rim of the porphyroblastic garnets are barroisite, ferrobarroisite, glaucophane and ferroglaucophanes and have higher Si 7.15-7.97 pfu, Na_B 0.60-1.96 pfu, X_{Mg} 0.13-0.87 and Al^{VI} 0.21-1.96 pfu than taramites in the core of the garnets (Fig. 4a-b). Amphiboles in albites (Amp2), epidotes (Amp3) and chlorites (Amp4) are ferroglaucophane with Si 7.38-7.83 pfu, Na_B 1.59-1.89 pfu, X_{Mg} 0.31-0.40 and Al^{VI} 1.45-1.62 (Fig. 4a). Amphiboles in the matrix (Amp5) are taramite, ferrobarroisite, katophorite, glaucophane and ferroglaucophane, have wide range of Si 6.40-7.98 pfu contents and similar Na_B 0.58-1.91 pfu, Al^{VI} 0.22-1.87 pfu and X_{Mg} 0.23-0.68 as amphibole (Amp1) inclusions in garnets (Fig. 4).

Discussion and Conclusions

There are several modes of occurrence of amphiboles in the garnet glaucophane schists, and they show a wide range of chemical compositions, i.e. sodic and sodic-calcic amphiboles, suggesting a diversity of their equilibrium P - T conditions.

Relict amphiboles of taramite (Amp1) as inclusions in the core of the porphyroblastic garnets have relatively high Al_2O_3 (<16.21 wt%) contents, indicating relatively high-temperature metamorphic conditions such as the amphibolite facies (Kabir and Takasu, 2013). The other amphiboles

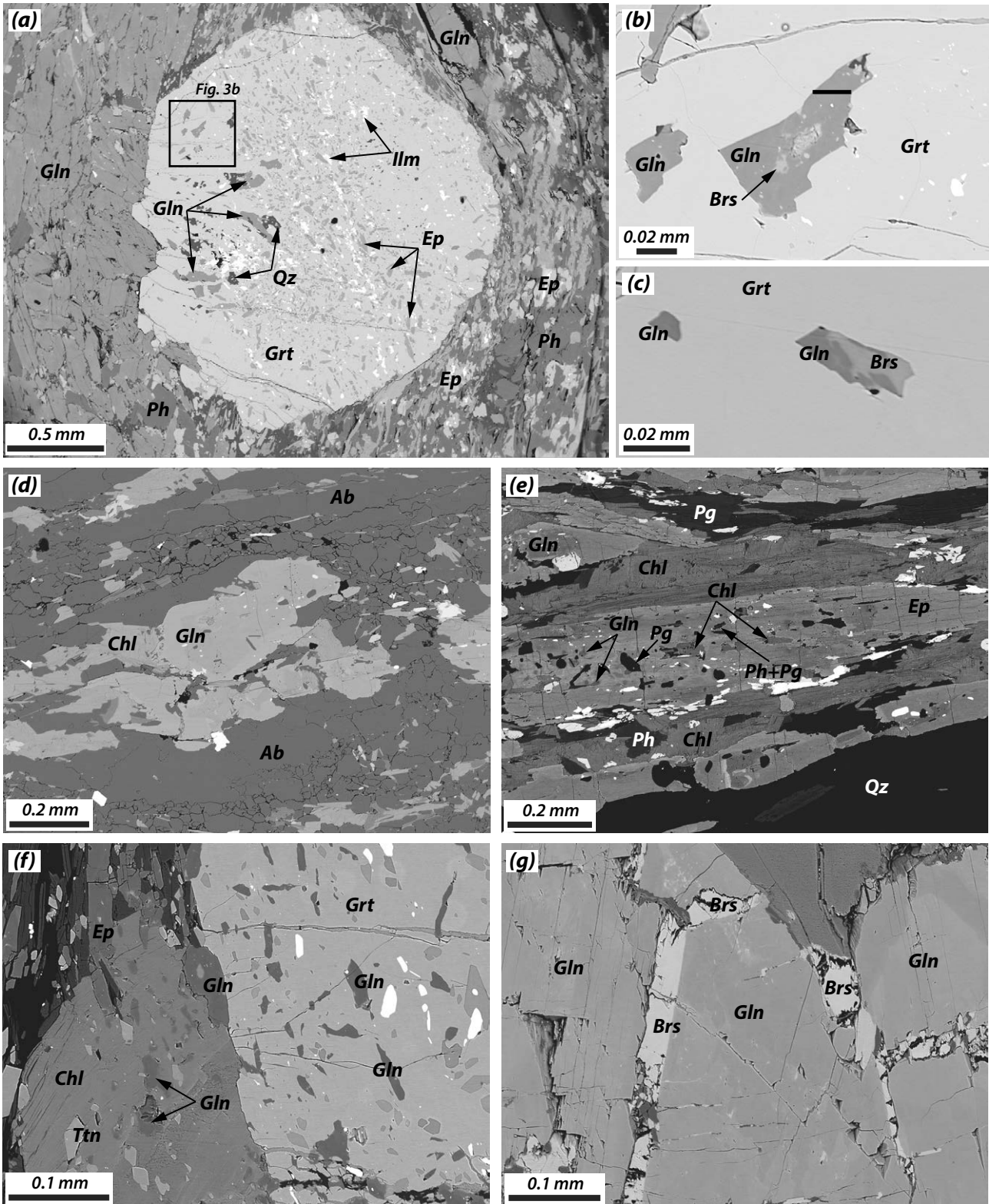


Fig. 3. Backscattered electron image (BEI) of garnet glaucophane schists from the Bizan area showing textural relationships of amphibole with other minerals. (a) Porphyroblastic garnet and schistosity-forming matrix minerals including amphibole (glaucophane) (Amp5), phengite and epidote. Porphyroblastic garnet contains inclusions of glaucophane (Amp1), epidote, ilmenite and quartz. (b-c) Porphyroblastic garnet contains inclusions of discrete grain of glaucophane (Amp1) and also barroisite core zoned to glaucophane rim. (d) Albite in the matrix contains inclusions of glaucophane (Amp2) and chlorite. (e) BEI of large-grained epidote contains inclusions of glaucophane (Amp3), phengite, paragonite and chlorite. Other matrix minerals of phengite, paragonite, chlorite and glaucophane (Amp5) also shown. (f) Chlorite in the matrix contains inclusions of glaucophane (Amp4) and titanite. (g) BEI showing matrix glaucophane (Amp5) is rimmed by barroisite.

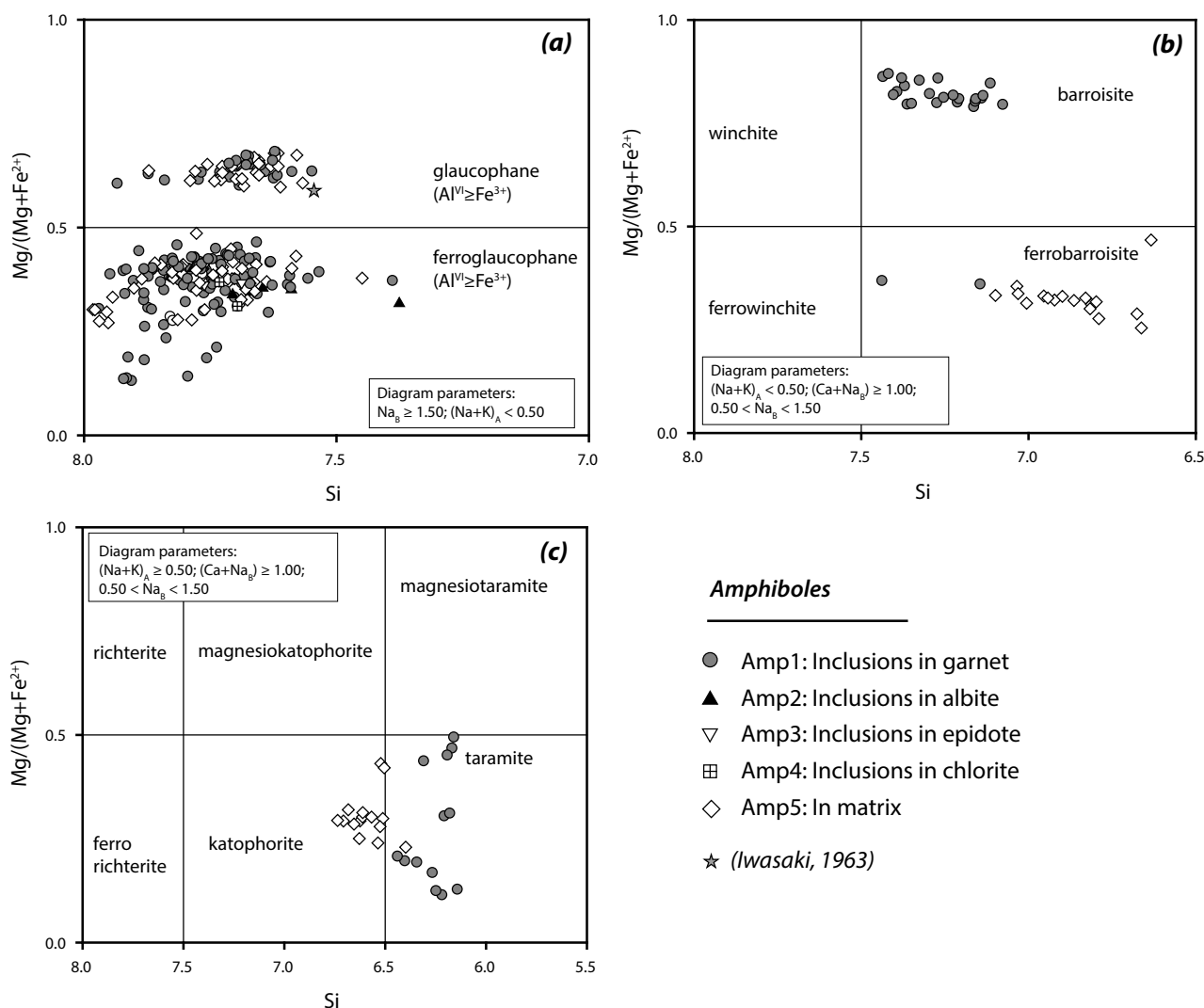


Fig. 4. Chemical compositions of amphiboles from the garnet glaucophane schists, star indicates the glaucophane composition of Iwasaki (1963).

as inclusions in the garnets (Amp1; ferroglaucophane, glaucophane, ferrobarrisite, barroisite) are the products of the prograde to the peak metamorphism (epidote-blueschist and eclogite facies metamorphic conditions). Amphiboles in the matrix (Amp5) represent a peak metamorphism of the eclogite facies (580-600°C and 18-20 kbar) (Kabir and Takasu, 2013). Amphiboles inclusions in the albite (Amp2), epidote (Amp3) and chlorite (Amp4) are probably a part of schistosity forming minerals, which correspond to the prograde to peak metamorphism of the eclogite facies.

Some glaucophanes in the matrix are rimmed by barroisite (Fig. 3g). These barroisites are probably developed during another prograde metamorphism at the epidote-amphibolite facies metamorphic conditions (Kabir and Takasu, 2013). This facies metamorphic event is correlated with the metamorphism of the albite-biotite zone of the Sambagawa metamorphism in the Besshi area (Enami *et al.*, 1994; Kabir and Takasu, 2010a, b).

Acknowledgements

We thank the members of the Metamorphic Geology Seminar of Shimane University for their discussion and helpful suggestions, and Hiroaki Komuro for critical reading and comments on the manuscript. Y. Kondo, M. Nakamura and M. Kainuma are thanked for providing field data. This study was partly supported by JSPS KAKENHI Grant (No. 24340123) to A.T.

References

- Aoya, M., 2001, *P-T-D* path of eclogite from the Sambagawa belt deduced from combination of petrological and microstructural analyses. *Journal of Petrology*, **42**, 1225-1248.
- Bence, A. E. and Albee, A. L., 1968, Empirical correction factors for the electron microanalysis of silicates and oxides. *Journal of Geology*, **76**, 382-403.
- Enami, M., 1983, Petrology of pelitic schists in the oligoclase-biotite zone of the Sambagawa metamorphic terrain, Japan: phase equilibria in the highest

- grade zone of a high-pressure intermediate type of metamorphic belt. *Journal of Metamorphic Geology*, **1**, 141-161.
- Enami, M., Wallis, S. R. and Banno, Y., 1994, Paragenesis of sodic pyroxene-bearing quartz schists: implications for the *P-T* history of the Sanbagawa belt. *Contributions to Mineralogy and Petrology*, **116**, 182-198.
- Endo, S. and Tsuboi, M., 2013, Petrogenesis and implications of jadeite-bearing kyanite eclogite from the Sanbagawa belt (SW Japan). *Journal of Metamorphic Geology*, **31**, 647-661.
- Faure, M., 1983, Eastward ductile shear during the early tectonic phase in the Sanbagawa belt. *Journal of the Geological Society of Japan*, **89**, 319-329.
- Higashino, T., 1975, Biotite zones of the Sanbagawa metamorphic terrain in the Shirayama area, central Shikoku. *Journal of the Geological Society of Japan*, **81**, 653-670 (in Japanese with English abstract).
- Higashino, T., 1990, The higher grade metamorphic zonation of the Sambagawa metamorphic belt in central Shikoku, Japan. *Journal of Metamorphic Geology*, **8**, 413-423.
- Iwasaki, M., 1963, Metamorphic rocks of the Kotu-Bizan area, eastern Shikoku. *Journal of the Faculty of Science, University of Tokyo, Section II*, **15**, 1-90.
- Kabir, M. F. and Takasu, A., 2010a, Evidence for multiple burial-partial exhumation cycles from the Onodani eclogites in the Sambagawa metamorphic belt, central Shikoku, Japan. *Journal of Metamorphic Geology*, **28**, 873-893.
- Kabir, M. F. and Takasu, A., 2010b, Glauconitic amphibole in the Seba eclogitic basic schists, Sambagawa metamorphic belt, central Shikoku, Japan: implications for timing of juxtaposition of the eclogite body with the non-eclogite Sambagawa schists. *Earth Sciences*, **64**, 183-192.
- Kabir, M. F. and Takasu, A., 2013, Jadeite-bearing garnet glaucophane schists in the Sambagawa metamorphic belt, Bizan area, eastern Shikoku, Japan: modes of occurrence and extent of eclogite distribution. Abstract of *X International Eclogite Conference* Courmayeur, Aosta Valley, Italy, p58.
- Kenzan Research Group, 1963, Geology of the crystalline schist region of Eastern Shikoku. *Earth Science*, **69**, 16-19 (in Japanese with English abstract).
- Kunugiza, K., Takasu, A. and Banno, S., 1986, The origin and metamorphic history of the ultramafic and metagabbro bodies in the Sanbagawa Metamorphic Belt. *Geological Society of America Memoir*, **164**, 375-386.
- Leake, B. E., Woolley, A. R., Arps, C. E. R., Birch, W. D., Gilbert, M. C., Grice, J. D., Hawthorne, F. C., Kato, A., Kisch, H. J., Krivovichev, V. G., Linthout, K., Laird, J., Mandarino, J. A., Maresch, W. V., Nickel, E. H., Rock, N. M. S., Schumacher, J. C., Smith, D. C., Stephenson, N. C. N., Ungaretti, L., Whittaker, E. J. W. and Youzhi, G., 1997, Nomenclature of amphiboles: report of the subcommittee on amphiboles of the International Mineralogical Association, Commission on New Minerals and Mineral Names. *The Canadian Mineralogist*, **35**, 219-246.
- Miyagi, Y. and Takasu, A., 2005, Prograde eclogites from the Tonaru epidote amphibolite mass in the Sambagawa Metamorphic Belt, central Shikoku, southwest Japan. *Island Arc*, **14**, 215-235.
- Miyamoto, A., Enami, M., Tsuboi, M. and Yokoyama, K., 2007, Peak conditions of kyanite-bearing quartz eclogites in the Sanbagawa metamorphic belt, central Shikoku, Japan. *Journal of Mineralogical and Petrological Sciences*, **102**, 352-367.
- Miyashiro, A., 1973, *Metamorphism and metamorphic belts*. George Allen and Unwin, London, England.
- Ota, T., Terabayashi, M. and Katayama, I., 2004, Thermobaric structure and metamorphic evolution of the Iratsu eclogite body in the Sanbagawa belt, central Shikoku, Japan. *Lithos*, **73**, 95-126.
- Takasu, A., 1989, *P-T* histories of peridotite and amphibolite tectonic blocks in the Sanbagawa metamorphic belt, Japan. In: *Evolution of Metamorphic Belts* (eds Daly, J. S., Cliff, R. A. & Yardley, B. W. D.), **43**, 533-538, Blackwell Scientific Publications, Oxford, Geological Society, London, Special Publications.
- Takasu, A., Wallis, S. R., Banno, S. and Dallmeyer, R. D., 1994, Evolution of the Sambagawa metamorphic belt, Japan. *Lithos*, **33**, 119-133.
- Wallis, S. R., 1998, Exhuming the Sanbagawa metamorphic belt: the importance of tectonic discontinuities. *Journal of Metamorphic Geology*, **16**, 83-95.
- Whitney, D. L. and Evans, B. W., 2010, Abbreviations for names of rock-forming minerals. *American Mineralogist*, **95**, 185-187.

(Received: Oct. 15, 2014, Accepted: Dec. 15, 2014)

(要 旨)

Kabir, Md. Fazle・高須 晃, 2014 四国東部眉山地域の三波川変成帯のざくろ石藍閃石片岩中の角閃石. 島根大学地球資源環境学研究所報告, **33**, 29-37.

眉山地域の三波川変成帯は泥質片岩, 塩基性片岩, 珪質片岩とともにまれにざくろ石藍閃石片岩を伴う。ざくろ石藍閃石片岩の主要鉱物はざくろ石と角閃石(藍閃石, 鉄藍閃石, バロワ閃石, カタフォル閃石, タラマ閃石)であるが, その他に少量の緑れん石, フェンジャイト, パラゴナイト, 緑泥石, 曹長石, チタン石, 石英を伴う。また, 単斜輝石(ひすい輝石-オンファス輝石), クロリトイド, ルチル, イルメナイト, 方解石, カリ長石, ジルコンが含まれることがある。角閃石には異なる5種類の産状がある。Amp1は斑状変晶ざくろ石中の包有物で, Na角閃石とNa-Ca角閃石(Amp1:鉄藍閃石, 藍閃石, バロワ閃石, フェロバロワ閃石, タラマ閃石)からなる。タラマ閃石質の角閃石は斑状変晶ざくろ石の核部に限って包有される。ざくろ石の縁部に包有される角閃石は累帯構造を示し, 核部はバロワ閃石, 縁部が藍閃石である。Amp2, Amp3, Amp4はそれぞれ曹長石, 緑れん石, 緑泥石中の包有物として産する角閃石で, いずれも鉄藍閃石の組成を示す。Amp5は基質部の角閃石で, 鉄藍閃石または藍閃石の組成を示す。Amp5には, 核部から縁部へ藍閃石からバロワ閃石へ累帯構造を示すものがある。このような角閃石の産状と化学組成の多様性は, ざくろ石藍閃石片岩に認められる3回の変成作用イベントに対応している。先駆的変成イベントは斑状変晶ざくろ石の核部に包有されるタラマ閃石質角閃石によって特徴づけられる。片理を形成する角閃石(鉄藍閃石, 藍閃石), 斑状変晶ざくろ石中の包有物(鉄藍閃石, 藍閃石, フェロバロワ閃石, バロワ閃石)と, 曹長石, 緑れん石, 緑泥石にそれぞれ包有される角閃石(鉄藍閃石)はエクロジャイト相変成イベントの昇温期からピーク期に形成されたと考えられる。また, 累帯構造をした角閃石の縁部のバロワ閃石は緑れん石角閃岩相変成イベントに形成されたと考えられる。

Table 1. Representative chemical compositions of amphiboles from the garnet glaucophane schists.

Sample	KB 1																			
Analysis	5	7	16	17	21	22	24	26	28	3	4	8	10	22	22	3	12	15	18	
Mode	In Grt	In Grt	In Grt	In Grt	In Grt	In Grt	In Grt	In Grt	In Grt	In Grt	In Grt	In Grt	In Grt	In Grt	In Grt	In Grt	In Grt	In Grt	In Grt	Matrix
	Amp1	Amp1	Amp1	Amp1	Amp1	Amp1	Amp1	Amp1	Amp1	Amp1	Amp1	Amp1	Amp1	Amp1	Amp1	Amp1	Amp1	Amp1	Amp1	Amp5
	Fgl	Fgl	Fgl	Fgl	Fgl	Fgl	Fgl	Fgl	Fgl	Fgl	Fgl	Fgl	Fgl	Fgl	Fgl	Fgl	Fgl	Fgl	Fgl	Fgl
SiO ₂	53.61	54.47	54.34	53.98	54.16	54.51	53.73	53.38	54.85	54.47	55.55	54.49	53.63	54.53	54.53	54.56	53.84	53.98	53.15	
TiO ₂	0.02	0.04	0.04	0.04	0.04	0.01	0.08	0.03	0.00	0.10	0.01	0.00	0.10	0.02	0.02	0.01	0.08	0.06	0.05	
Al ₂ O ₃	10.16	10.48	10.24	10.16	10.11	9.39	9.75	9.81	10.22	10.34	10.12	10.57	11.10	10.67	10.67	10.15	11.04	10.11	9.40	
Fe ₂ O ₃	4.03	4.27	3.77	4.86	5.42	7.25	5.59	5.43	3.83	4.32	3.61	3.48	4.25	4.88	4.88	3.68	5.56	5.92	6.80	
FeO	16.67	14.83	15.00	14.38	14.40	13.39	14.40	14.46	14.83	14.39	14.75	17.64	15.99	15.25	15.25	15.22	12.69	13.70	14.02	
MnO	0.11	0.37	0.16	0.33	0.28	0.27	0.24	0.24	0.15	0.38	0.49	0.32	0.42	0.39	0.39	0.05	0.35	0.26	0.17	
MgO	4.49	5.30	5.68	5.45	5.43	5.76	5.53	5.43	5.60	5.42	5.50	3.56	4.53	4.80	4.80	5.35	6.29	5.61	5.47	
CaO	0.94	0.56	0.72	0.80	0.52	0.56	0.85	0.85	0.35	0.70	0.37	0.41	0.97	0.53	0.53	0.37	0.91	0.71	0.98	
Na ₂ O	6.85	7.13	7.22	6.88	7.20	6.96	6.94	6.93	7.31	6.79	7.10	6.94	6.96	7.06	7.06	7.21	7.09	6.87	6.72	
K ₂ O	0.04	0.02	0.03	0.02	0.00	0.02	0.03	0.03	0.02	0.03	0.01	0.02	0.06	0.05	0.05	0.02	0.03	0.02	0.03	
Cr ₂ O ₃	0.00	0.00	0.00	0.01	0.00	0.00	0.01	0.03	0.00	0.00	0.00	0.00	0.03	0.01	0.01	0.04	0.01	0.00	0.04	
Total	96.92	97.47	97.20	96.91	97.56	98.12	97.15	96.62	97.16	96.94	97.51	97.43	98.04	98.18	98.18	96.67	97.88	97.23	96.83	
O	23	23	23	23	23	23	23	23	23	23	23	23	23	23	23	23	23	23	23	
Si	7.80	7.81	7.81	7.79	7.78	7.78	7.76	7.76	7.87	7.83	7.92	7.88	7.70	7.79	7.79	7.87	7.66	7.76	7.73	
Ti	0.00	0.00	0.00	0.00	0.00	0.00	0.01	0.00	0.00	0.01	0.00	0.00	0.01	0.00	0.00	0.00	0.01	0.01	0.01	
Al ^{IV}	0.20	0.19	0.19	0.21	0.22	0.22	0.24	0.24	0.13	0.17	0.08	0.12	0.30	0.21	0.21	0.13	0.34	0.24	0.27	
Al ^{VI}	1.54	1.58	1.55	1.52	1.49	1.36	1.42	1.44	1.59	1.58	1.62	1.68	1.58	1.58	1.58	1.60	1.51	1.47	1.34	
Fe ³⁺	0.42	0.44	0.39	0.51	0.56	0.75	0.59	0.57	0.40	0.45	0.37	0.36	0.44	0.50	0.50	0.38	0.58	0.62	0.72	
Fe ²⁺	2.05	1.80	1.82	1.76	1.75	1.63	1.76	1.78	1.79	1.75	1.77	2.15	1.94	1.84	1.84	1.85	1.53	1.67	1.73	
Mn	0.01	0.04	0.02	0.04	0.03	0.03	0.03	0.03	0.02	0.05	0.06	0.04	0.05	0.05	0.05	0.01	0.04	0.03	0.02	
Mg	0.97	1.13	1.22	1.17	1.16	1.23	1.19	1.18	1.20	1.16	1.17	0.77	0.97	1.02	1.02	1.15	1.33	1.20	1.19	
Ca	0.15	0.09	0.11	0.12	0.08	0.09	0.13	0.13	0.05	0.11	0.06	0.06	0.15	0.08	0.08	0.06	0.14	0.11	0.15	
Na ^B	1.85	1.91	1.89	1.88	1.92	1.91	1.87	1.87	1.95	1.89	1.94	1.94	1.85	1.92	1.92	1.94	1.86	1.89	1.85	
Na ^A	0.08	0.07	0.12	0.05	0.09	0.01	0.07	0.08	0.09	0.00	0.02	0.01	0.09	0.03	0.03	0.08	0.09	0.02	0.05	
K	0.01	0.00	0.00	0.00	0.00	0.00	0.01	0.01	0.00	0.01	0.00	0.00	0.01	0.01	0.01	0.00	0.01	0.00	0.01	
Cr	0.00	0.00	0.00	0.00	0.00	0.00	0.00	0.00	0.00	0.00	0.00	0.00	0.00	0.00	0.00	0.00	0.00	0.00	0.00	
Total	15.09	15.07	15.13	15.05	15.09	15.02	15.08	15.09	15.09	15.01	15.02	15.01	15.10	15.04	15.04	15.08	15.10	15.03	15.05	
X _{Mg}	0.32	0.39	0.40	0.40	0.40	0.43	0.40	0.40	0.40	0.40	0.40	0.26	0.33	0.36	0.36	0.38	0.47	0.42	0.41	

Sample	KB 1																			
Analysis	19	38	39	46	30	31	32	46	47	54	55	82	91	92	92	75	76	77	78	
Mode	In Grt	Matrix	Matrix	In Ab	Matrix	Matrix	Matrix	Matrix	Matrix	Matrix	Matrix	In Grt	In Grt	In Grt	In Grt	In Grt	In Grt	In Grt	In Grt	Matrix
	Amp1	Amp5	Amp2	Amp5	Amp5	Amp5	Amp5	Amp5	Amp5	Amp5	Amp5	Amp1	Amp1	Amp1	Amp1	Amp1	Amp1	Amp1	Amp1	Amp1
	Fgl	Fgl	Fgl	Fgl	Gln	Gln	Gln	Gln	Gln	Gln	Gln	Gln	Gln	Gln	Gln	Gln	Gln	Gln	Gln	Gln
SiO ₂	53.62	54.39	54.21	54.32	54.20	54.69	54.93	53.67	53.41	54.23	54.16	53.98	55.05	53.84	54.01	53.76	53.68	54.24	54.10	
TiO ₂	0.04	0.08	0.05	0.01	0.06	0.08	0.03	0.10	0.07	0.04	0.06	0.13	0.05	0.10	0.04	0.07	0.04	0.04	0.02	
Al ₂ O ₃	10.60	10.26	10.36	10.54	9.75	9.80	9.82	8.83	8.81	9.00	9.18	9.06	9.13	8.33	10.04	9.96	9.79	9.78	10.00	
Fe ₂ O ₃	4.62	4.80	6.28	3.86	5.59	4.97	6.20	6.62	7.33	7.49	7.05	7.01	5.73	8.07	6.61	6.27	7.47	7.68	5.97	
FeO	15.54	14.28	13.92	15.02	9.49	9.37	8.93	9.51	9.03	8.16	8.60	8.86	9.35	8.87	8.27	8.73	8.30	7.97	8.94	
MnO	0.09	0.16	0.18	0.13	0.09	0.07	0.11	0.08	0.13	0.05	0.11	0.05	0.04	0.13	0.05	0.07	0.10	0.11	0.09	
MgO	4.84	5.58	5.69	5.28	9.52	9.40	9.61	9.35	9.48	9.53	9.50	9.65	9.27	9.53	9.34	9.49	9.62	9.58	9.37	
CaO	0.97	0.71	0.97	0.71	2.29	1.75	1.84	2.16	2.40	1.65	1.82	2.18	1.52	2.55	1.18	1.52	1.70	1.30	1.12	
Na ₂ O	6.72	6.83	6.86	6.88	6.49	6.64	6.75	6.50	6.32	6.50	6.58	6.45	6.58	6.01	7.08	7.16	7.06	7.18	7.49	
K ₂ O	0.06	0.05	0.04	0.04	0.14	0.10	0.09	0.11	0.13	0.10	0.11	0.13	0.10	0.10	0.07	0.07	0.08	0.06	0.08	
Cr ₂ O ₃	0.04	0.00	0.01	0.00	0.00	0.01	0.02	0.00	0.03	0.02	0.03	0.00	0.00	0.01	0.00	0.00	0.01	0.01	0.03	
Total	97.12	97.15	98.55	96.79	97.61	96.87	98.32	96.93	97.12	96.75	97.19	97.51	96.81	97.54	96.69	97.08	97.84	97.96	97.21	
O	23	23	23	23	23	23	23	23	23	23	23	23	23	23	23	24	25	26	27	
Si	7.75	7.81	7.71	7.83	7.65	7.73	7.67	7.66	7.62	7.70	7.67	7.64	7.79	7.65	7.65	7.62	7.57	7.61	7.65	
Ti	0.00	0.01	0.01	0.00	0.01	0.01	0.00	0.01	0.01	0.00	0.01	0.01	0.01	0.01	0.00	0.01	0.00	0.00	0.00	
Al ^{IV}	0.25	0.19	0.29	0.17	0.35	0.27	0.33	0.34	0.38	0.30	0.33	0.36	0.21	0.35	0.35	0.38	0.43	0.39	0.35	
Al ^{VI}	1.56	1.54	1.44	1.62	1.27	1.36	1.29	1.15	1.10	1.20	1.20	1.15	1.32	1.04	1.33	1.28	1.19	1.23	1.32	
Fe ³⁺	0.48	0.50	0.65	0.40	0.58	0.52	0.64	0.69	0.77	0.78	0.73	0.73	0.60	0.84	0.69	0.65	0.78	0.79	0.62	
Fe ²⁺	1.90	1.73	1.68	1.83	1.13	1.12	1.06	1.15	1.10	0.99	1.04	1.07	1.12	1.07	1.00	1.05	0.99	0.95	1.07	
Mn	0.01	0.02	0.02	0.02	0.01	0.01	0.01	0.01	0.02	0.01	0.01	0.01	0.00	0.02	0.01	0.01	0.01	0.01	0.01	
Mg	1.04	1.19	1.20	1.14	2.00	1.98	2.00	1.99	2.01	2.02	2.00	2.04	1.96	2.02	1.97	2.00	2.02	2.00	1.98	
Ca	0.15	0.11	0.15	0.11	0.35	0.26	0.28	0.33	0.37	0.25	0.28	0.33	0.23	0.39	0.18	0.23	0.26	0.19	0.17	
Na ^B	1.85	1.89	1.85	1.89	1.65	1.74	1.72	1.67	1.63	1.75	1.72	1.67	1.77	1.61	1.82	1.77	1.74	1.81	1.83	
Na ^A	0.03	0.01	0.04	0.03	0.12	0.09	0.10	0.13	0.11	0.04	0.08	0.10	0.04	0.04	0.12	0.20	0.19	0.15	0.22	
K	0.01	0.01	0.01	0.01	0.02	0.02	0.02	0.02	0.02	0.02	0.02	0.02	0.02	0.02	0.01	0.01	0.01	0.01	0.01	
Cr	0.00	0.00	0.00	0.00	0.00	0.00	0.00	0.00	0.00	0.00	0.00	0.00	0.00	0.00	0.00	0.00	0.00	0.00	0.00	
Total	15.05	15.02	15.05	15.04	15.15	15.10	15.12	15.15	15.14	15.06	15.10	15.12	15.05	15.06	15.14	15.21	15.20	15.16	15.24	
X _{Mg}	0.35	0.41	0.42	0.38	0.64	0.64	0.65	0.63	0.65	0.67	0.66	0.66	0.64	0.65	0.66	0.66	0.67	0.68	0.65	

Table 1. (continued)

Sample	KB 1																		
Analysis	10	11	12	13	19	3	5	14	24	26	28	2	4	5	18	30	25	27	28
Mode	Matrix	Matrix	Matrix	Matrix	In Grt	Matrix	Matrix	In Grt	In Grt	In Grt	Matrix	In Grt	In Grt	In Grt	Matrix	Matrix	In Ab	In Ab	In Chl
	Amp5	Amp5	Amp5	Amp5	Amp1	Amp5	Amp5	Amp1	Amp1	Amp1	Amp5	Amp1	Amp1	Amp1	Amp5	Amp5	Amp2	Amp2	Amp4
	Fgl	Fgl	Fgl	Fgl	Fgl	Fgl	Fgl	Fgl	Fgl	Fgl	Fgl	Fgl	Fgl	Fgl	Trm	Fgl	Fgl	Fgl	Fgl
	Core									Rim									
SiO ₂	54.25	54.42	54.39	54.62	53.96	55.27	53.28	53.98	53.72	54.38	55.42	53.72	54.35	40.86	54.60	55.19	52.75	51.94	52.84
TiO ₂	0.04	0.10	0.06	0.00	0.09	0.01	0.10	0.06	0.06	0.05	0.07	0.09	0.08	0.25	0.01	0.03	0.12	0.02	0.09
Al ₂ O ₃	9.40	10.22	9.71	10.65	10.22	10.58	11.65	9.83	10.99	10.28	10.73	11.31	10.19	15.17	11.02	10.03	11.23	11.17	10.90
Fe ₂ O ₃	5.23	4.82	3.41	1.80	3.65	2.40	3.59	4.32	2.80	4.21	1.71	3.09	3.52	5.26	1.31	4.40	4.23	5.01	4.22
FeO	14.30	14.47	15.61	17.96	15.15	17.01	16.18	15.10	15.76	15.42	16.94	14.73	15.03	19.85	17.62	15.61	15.63	15.42	15.86
MnO	0.18	0.20	0.19	0.11	0.21	0.07	0.13	0.15	0.06	0.17	0.03	0.21	0.08	0.26	0.10	0.16	0.08	0.10	0.09
MgO	5.67	5.31	5.34	3.78	5.29	4.17	4.46	5.53	5.44	5.20	4.77	6.01	5.61	2.69	3.78	4.87	4.88	4.74	4.61
CaO	0.56	0.53	0.69	0.27	0.81	0.30	1.16	0.82	1.36	0.73	0.40	1.48	0.68	7.53	0.30	0.34	1.58	1.37	0.93
Na ₂ O	7.01	6.88	7.02	7.05	6.86	6.78	6.69	7.09	6.83	7.04	7.14	6.96	7.09	4.38	6.79	6.97	6.44	6.77	6.91
K ₂ O	0.03	0.03	0.03	0.01	0.02	0.01	0.07	0.01	0.05	0.02	0.02	0.04	0.01	0.35	0.03	0.01	0.08	0.07	0.04
Cr ₂ O ₃	0.01	0.04	0.06	0.03	0.10	0.02	0.01	0.03	0.00	0.03	0.00	0.02	0.00	0.00	0.04	0.00	0.02	0.03	0.00
Total	96.67	97.01	96.51	96.28	96.36	96.59	97.33	96.91	97.06	97.52	97.21	97.63	96.66	96.60	95.59	97.61	97.04	96.64	96.47
O	23	23	23	23	23	23	23	23	23	23	23	23	23	23	23	23	23	23	23
Si	7.85	7.83	7.89	7.95	7.83	7.98	7.69	7.81	7.75	7.81	7.94	7.68	7.84	6.34	7.97	7.90	7.65	7.59	7.71
Ti	0.00	0.01	0.01	0.00	0.01	0.00	0.01	0.01	0.01	0.01	0.01	0.01	0.01	0.03	0.00	0.00	0.01	0.00	0.01
Al ^{IV}	0.15	0.17	0.11	0.05	0.17	0.02	0.31	0.19	0.25	0.19	0.06	0.32	0.16	1.66	0.03	0.10	0.35	0.41	0.29
Al ^{VI}	1.45	1.56	1.54	1.78	1.57	1.78	1.67	1.48	1.61	1.55	1.76	1.59	1.58	1.12	1.87	1.59	1.56	1.51	1.58
Fe ³⁺	0.55	0.50	0.36	0.19	0.38	0.25	0.37	0.45	0.29	0.44	0.18	0.32	0.37	0.58	0.14	0.46	0.44	0.53	0.44
Fe ²⁺	1.75	1.76	1.91	2.20	1.85	2.06	1.97	1.84	1.91	1.87	2.04	1.77	1.83	2.61	2.16	1.89	1.91	1.91	1.95
Mn	0.02	0.02	0.02	0.01	0.03	0.01	0.02	0.02	0.01	0.02	0.00	0.03	0.01	0.03	0.01	0.02	0.01	0.01	0.01
Mg	1.22	1.14	1.15	0.82	1.14	0.90	0.96	1.19	1.17	1.11	1.02	1.28	1.21	0.62	0.82	1.04	1.05	1.03	1.00
Ca	0.09	0.08	0.11	0.04	0.13	0.05	0.18	0.13	0.21	0.11	0.06	0.23	0.10	1.25	0.05	0.05	0.25	0.21	0.14
Na ^B	1.91	1.92	1.89	1.96	1.87	1.90	1.82	1.87	1.79	1.89	1.94	1.77	1.90	0.75	1.92	1.93	1.75	1.79	1.86
Na ^A	0.05	0.00	0.08	0.03	0.06	0.00	0.05	0.11	0.12	0.07	0.05	0.16	0.09	0.57	0.00	0.00	0.06	0.13	0.10
K	0.00	0.00	0.00	0.00	0.00	0.00	0.01	0.00	0.01	0.00	0.00	0.01	0.00	0.07	0.00	0.00	0.02	0.01	0.01
Cr	0.00	0.00	0.01	0.00	0.01	0.00	0.00	0.00	0.00	0.00	0.00	0.00	0.00	0.00	0.00	0.00	0.00	0.00	0.00
Total	15.06	15.00	15.09	15.03	15.06	14.94	15.06	15.12	15.13	15.08	15.05	15.16	15.09	15.64	14.97	14.99	15.07	15.14	15.11
X _{Mg}	0.41	0.39	0.38	0.27	0.38	0.30	0.33	0.39	0.38	0.37	0.33	0.42	0.40	0.19	0.28	0.35	0.36	0.35	0.34

Sample	BZ B/PRE 7																		
Analysis	13	14	15	17	18	44	79	7	38	47	35	36	37	2	5	13	14	15	16
Mode	In Grt	Matrix	In Grt	In Grt	In Grt	In Grt	Matrix	In Grt	In Grt	In Grt	Matrix	Matrix	Matrix	In Grt	In Ep	Matrix	Matrix	Matrix	Matrix
	Amp1	Amp5	Amp1	Amp1	Amp1	Amp1	Amp5	Amp1	Amp1	Amp1	Amp5	Amp5	Amp5	Amp5	Amp1	Amp5	Amp5	Amp5	Amp5
	Fbrs	Fgl	Fgl	Fbrs	Fgl	Fgl	Fgl	Trm	Trm	Trm	Fbrs	Ktp	Ktp	Fbrs	Fgl	Ktp	Ktp	Trm	Fbrs
SiO ₂	47.80	53.57	54.10	49.19	53.58	54.83	53.32	41.20	41.11	41.26	45.19	43.80	43.81	44.99	53.32	43.17	42.28	41.46	46.54
TiO ₂	0.13	0.08	0.00	0.13	0.09	0.05	0.01	0.28	0.23	0.07	0.35	0.39	0.44	0.00	0.04	0.08	0.08	0.09	0.04
Al ₂ O ₃	8.18	9.35	9.33	4.29	10.26	9.45	10.84	16.21	15.42	16.02	13.68	14.67	15.18	7.37	10.16	11.54	11.64	12.09	7.30
Fe ₂ O ₃	9.61	8.03	6.75	12.51	6.50	6.29	4.11	5.27	6.97	6.29	7.48	4.44	4.10	11.03	4.94	7.89	8.38	9.07	10.95
FeO	16.42	12.71	13.81	16.19	13.25	14.17	17.00	13.29	13.60	13.99	13.25	15.22	15.39	17.82	15.29	19.35	19.51	19.63	16.94
MnO	0.40	0.16	0.32	0.38	0.21	0.07	0.07	0.41	0.44	0.26	0.12	0.13	0.17	0.29	0.10	0.26	0.20	0.29	0.22
MgO	5.38	5.93	5.68	5.54	5.82	5.64	3.72	7.38	6.81	6.54	6.71	6.52	6.31	4.87	4.94	3.67	3.50	3.33	4.94
CaO	6.21	0.68	0.70	5.59	1.10	0.70	0.70	8.40	8.53	7.94	7.41	7.97	8.05	7.37	0.79	7.56	7.68	8.21	7.46
Na ₂ O	3.96	6.88	7.00	3.84	6.60	6.76	6.73	4.64	4.48	5.18	3.82	4.25	4.14	3.54	6.90	3.80	3.79	3.53	2.31
K ₂ O	0.24	0.03	0.02	0.05	0.04	0.05	0.02	0.78	0.38	0.09	0.21	0.23	0.23	0.48	0.04	0.76	0.91	1.08	0.71
Cr ₂ O ₃	0.00	0.03	0.01	0.00	0.00	0.00	0.00	0.00	0.00	0.02	0.04	0.01	0.00	0.01	0.02	0.00	0.00	0.00	0.00
Total	98.33	97.44	97.73	97.71	97.45	98.00	96.51	97.86	97.98	97.65	98.26	97.63	97.82	97.78	96.55	98.09	97.97	98.77	97.41
O	23	23	23	23	23	23	23	23	23	23	23	23	23	23	23	23	23	23	23
Si	7.15	7.71	7.77	7.45	7.69	7.83	7.79	6.16	6.17	6.19	6.64	6.52	6.51	6.93	7.76	6.63	6.54	6.40	7.11
Ti	0.02	0.01	0.00	0.01	0.01	0.00	0.00	0.03	0.03	0.01	0.04	0.04	0.05	0.00	0.00	0.01	0.01	0.01	0.00
Al ^{IV}	0.85	0.29	0.23	0.55	0.31	0.17	0.21	1.84	1.83	1.81	1.36	1.48	1.49	1.07	0.24	1.37	1.46	1.60	0.89
Al ^{VI}	0.60	1.30	1.35	0.21	1.43	1.42	1.65	1.02	0.90	1.03	1.01	1.10	1.16	0.27	1.51	0.72	0.66	0.60	0.42
Fe ³⁺	1.04	0.84	0.70	1.36	0.68	0.65	0.43	0.57	0.76	0.68	0.80	0.48	0.44	1.22	0.52	0.86	0.92	1.00	1.20
Fe ²⁺	2.10	1.56	1.69	2.11	1.61	1.72	2.10	1.68	1.74	1.78	1.66	1.92	1.93	2.36	1.88	2.53	2.57	2.59	2.22
Mn	0.05	0.02	0.04	0.05	0.03	0.01	0.01	0.05	0.06	0.03	0.02	0.02	0.02	0.04	0.01	0.03	0.03	0.04	0.03
Mg	1.20	1.27	1.22	1.25	1.25	1.20	0.81	1.64	1.52	1.46	1.47	1.45	1.40	1.12	1.07	0.84	0.81	0.77	1.12
Ca	1.00	0.10	0.11	0.91	0.17	0.11	0.11	1.35	1.37	1.28	1.17	1.27	1.28	1.22	0.12	1.24	1.27	1.36	1.22
Na ^B	1.00	1.90	1.89	1.09	1.83	1.87	1.89	0.65	0.63	0.72	0.83	0.73	0.72	0.78	1.88	0.76	0.73	0.64	0.68
Na ^A	0.14	0.02	0.06	0.03	0.01	0.00	0.01	0.69	0.68	0.78	0.26	0.50	0.47	0.27	0.07	0.38	0.41	0.42	0.00
K	0.05	0.00	0.00	0.01	0.01	0.01	0.00	0.15	0.07	0.02	0.04	0.04	0.04	0.09	0.01	0.15	0.18	0.21	0.14
Cr	0.00	0.00	0.00	0.00	0.00	0.00	0.00	0.00	0.00	0.00	0.00	0.00	0.00	0.00	0.00	0.00	0.00	0.00	0.00
Total	15.19	15.03	15.06	15.04	15.01	14.99	15.02	15.84	15.75	15.80	15.30	15.54	15.51	15.37	15.08	15.52	15.59	15.63	15.04
X _{Mg}	0.36	0.45	0.42	0.37	0.44	0.41	0.28	0.49	0.47	0.45	0.47	0.43	0.42	0.32	0.36	0.25	0.24	0.23	0.34

